OBSERVATION OF AMPERE FORCES IN MERCURY

T.E. PHIPPS and T.E. PHIPPS Jr.
908 South Busey Avenue, Urbana, IL 61801, USA

Received 10 October 1989; revised manuscript received 20 February 1990; accepted for publication 21 February 1990
Communicated by J.P. Vigier

An experiment proposed by Wesley involving passing current through a mercury cell of varying cross section has been performed and appears to confirm the existence of Ampère tension (Ampère longitudinal forces).

1. Background

A question originating in the earliest days of classical electrodynamics concerning the applicability of Newton's third law (equality and collinearity of action–reaction) to the interaction of nonrelativistic "current elements" has never been empirically resolved. The first investigator, Ampère, devised and observationally supported a law that conformed to Newton's third law. Written in terms of electric current densities J_1, J_2, Ampère's law [1] for the differential of ponderomotive force in dynes exerted by conductive volume element d^3r_1 on element d^3r_2 is

$$d^6F_{2,A} = \frac{d^3r_1\, d^3r_2}{r_{12}^3}\, r_{12}[-2J_1\cdot J_2 + 3(J_1\cdot r_{12})(J_2\cdot r_{12})/r_{12}^2]\,, \qquad (1)$$

where current is in abamperes and r_{12} is the position vector from element 1 to 2. Later investigators [2], beginning with Grassmann and continuing with Biot, Savart, Riemann, Lorentz, Heaviside, etc., questioned the need to honor Newton's third law in other than an integrated sense. They felt free to add to Ampere's law any exact differential – since this integrates to zero around any closed circuit external to the test element and thus can introduce no observable distinction. It is worth pointing out that one of Newton's basic assertions about forces between bodies, the equality of action and reaction, has almost no place in relativistic mechanics.

But consider action–reaction within a single circuit: If the test element (e.g., in Ampère's case a wire floating in mercury cups) forms a finite current-carrying segment that is mechanically decoupled from (or very loosely coupled to) the remainder of its own circuit, then the observable motions of the test element are uninfluenced by currents flowing within itself (which in acting upon each other exert only internal stresses without ponderomotive "bootstrap-lifting"). *Observable motions* of the test element can thus be produced *only* by the action upon it of currents flowing in the *external partial circuit*. An exact differential integrated around a partial circuit does not in general yield zero. Hence in principle there should exist experimental possibilities to resolve the choice among the infinitude of force-law options distinguished only by an additive exact differential. Contrary theoretical claims [3,4] result from integrating around the full circuit, hence from ignoring the observability requirement just mentioned.

2. Wesley's mercury experiment

An experiment concerned with the choice in question, proposed by Wesley [5], has been performed. Since Ampère's law, eq. (1), predicts longitudinal forces [1] of repulsion between collinear current elements, whereas Lorentz's law predicts none, Wesley suggested seeking evidence of the existence of this "Ampère tension" in the behavior of current-carrying liquid mercury. Specifically, he proposed passing direct current through a wedge-shaped mercury

cell and observing its effect on the meniscus heights in two vertical tubes located at positions of different current density, as shown in fig. 1, wherein the cell used in the presently reported experiment is sketched.

If w_A^2 denotes the (square) cross sectional area of mercury transverse to current flow in the vicinity of tube A in fig. 1, w_B^2 the same at tube B, then an Ampère pressure (tension) difference $\Delta P = F_B/w_B^2 - F_A/w_A^2$ arises according to eq. (1), where the F's are longitudinal ponderomotive Ampère forces exerted by current flowing in the fixed external partial circuit upon the contents of the cell. This pressure difference can be considered to produce an "Ampère driving force" $F_d = \pi r_1^2 \Delta P = k_2 I^2$ acting upon the mercury in the vertical tubes of inner radius r_1 and within the region of the cell connecting those tubes. By integration eq. (1) for idealized simple geometry, Wesley [5] obtained a closed-form result,

$$k_2 = \frac{\pi r_1^2}{100}\left(\frac{C' + \ln(L_0/w_B)}{w_B^2} - \frac{C' + \ln(L_0/w_A)}{w_A^2}\right), \tag{2}$$

which serves as an approximation for our actual geometry. Here L_0 is the side length of the (assumed square) circuit containing the mercury cell, C' is a constant shown [5] to have the value 1.03107, and abamps are replaced by amps. In our experiment $L_0 = 12.5$ cm, $w_A = 4.57$ cm, $w_B = 3.05$ cm, $r_1 = 0.54$ cm; consequently

$$k_2 = 0.001511\,, \tag{3a}$$

a value to be used in the equation

$$\text{rms force in dynes} = k_2 I^2\,, \tag{3b}$$

where I is rms current in amperes. Internal stresses produced by interactions among current elements within the cell could also affect the observable mercury levels in the tubes – but only to the extent that mercury is compressible. To first approximation we may treat mercury as incompressible and neglect such effects.

3. ac version of the experiment

Suppose that sinusoidally alternating current (ac) of angular frequency $\omega/2$ is applied to the electrodes

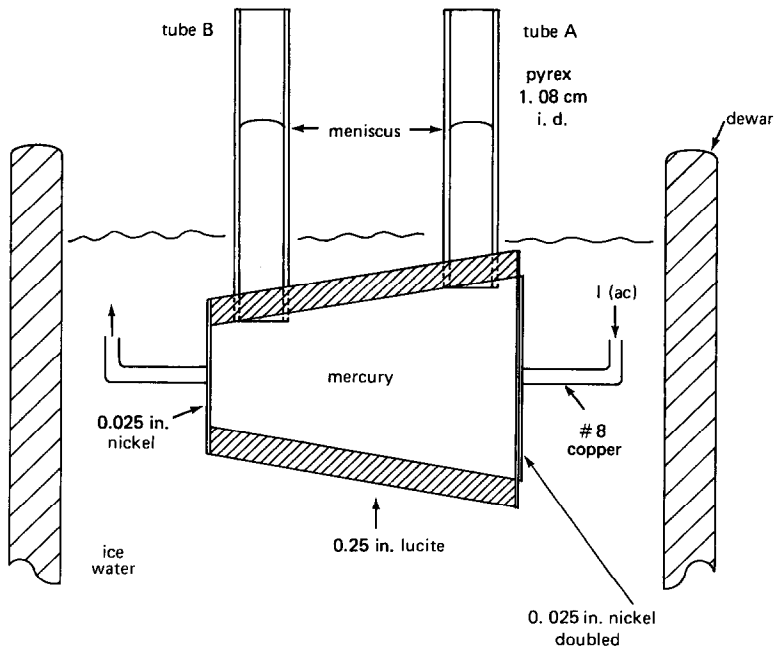

Fig. 1. Sketch of lucite cell with sheet nickel electrodes used as mercury container in the experiment.

at the two ends of the mercury cell in fig. 1, $I_t = I_0 \cos(\omega t/2)$. We have

$$F_\alpha(t) = k_2 I_t^2 = k_2 I_0^2 \cos^2(\omega t/2)$$
$$= \tfrac{1}{2} k_2 I_0^2 (1 + \cos \omega t) .$$

The oscillatory part of this force produces a harmonic mechanical driving force

$$F_d = \tfrac{1}{2} k_2 I_0^2 \cos \omega t = k_2 I^2 \cos \omega t . \quad (4)$$

The mechanical frequency $f = \omega/2\pi$ is twice the electrical excitation frequency as a result of the square law, eq. (3b). (For any I^2 law the direction or sign of current makes no difference, so there are two force pulses per electrical cycle.)

Let z measure mercury meniscus height above equilibrium level. The equation of motion of a mass m of mercury is

$$m\ddot{z} + R\dot{z} + Kz = F_d = k_2 I^2 \cos \omega t , \quad (5)$$

where R measures the effect of energy dissipation and K is proportional to restoring force (gravity). The motion in question is a "swinging" between tubes of some portion of the total mercury mass contained in the cell. We do not attempt to treat the fluid dynamics, but limit ourselves to inferences from observational data. This damped, driven harmonic oscillator has a solution [6] that when time-averaged over a cycle yields rms vertical displacement from equilibrium of

$$z_{rms} = \frac{k_2 I^2}{2\sqrt{R^2\omega^2 + (m\omega^2 - K)^2}} . \quad (6)$$

An observed (amplified) rms electrical signal S, designed to measure meniscus departure from equilibrium, will obey $S = k_1 z_{rms}$, where k_1 is a constant to be determined by some calibration procedure. This signal will also obey $S = bI^2$, where the slope parameter is a function of frequency, $b = b(f)$. Combining these results, we get

$$b(f) = \frac{S}{I^2} = \frac{a_1}{\sqrt{a_2 f^2 + (f^2 - a_3)^2}} , \quad (7a)$$

$$a_1 = \frac{k_1 k_2}{8\pi^2 m}, \quad a_2 = \frac{R^2}{4\pi^2 m^2}, \quad a_3 = f_0^2 = \frac{K}{4\pi^2 m} , \quad (7b)$$

which describes a resonance with peak near frequency f_0.

To generate this electrical signal optical amplification is employed, as indicated in fig. 2. This permits observation of the micron-sized meniscus oscillations predicted (for moderate currents) by eqs. (3), (6). He–Ne laser light, focused in the vicinity of tube A or B (these tubes being transparent), is partly shadowed by the meniscus and is detected by a photodiode, the output of which passes via a load resistor to the A or B preamplifier channel of a lock-in amplifier (LIA) tuned to frequency f of eq. (7). (This f, as noted, is the mechanical oscillation frequency of the mercury system, equal to twice the frequency of electrical current applied to the cell.) By phase comparison of the A and B channel LIA signals it is verified that the coherent signals detected are 180 degrees out of phase, corresponding to a

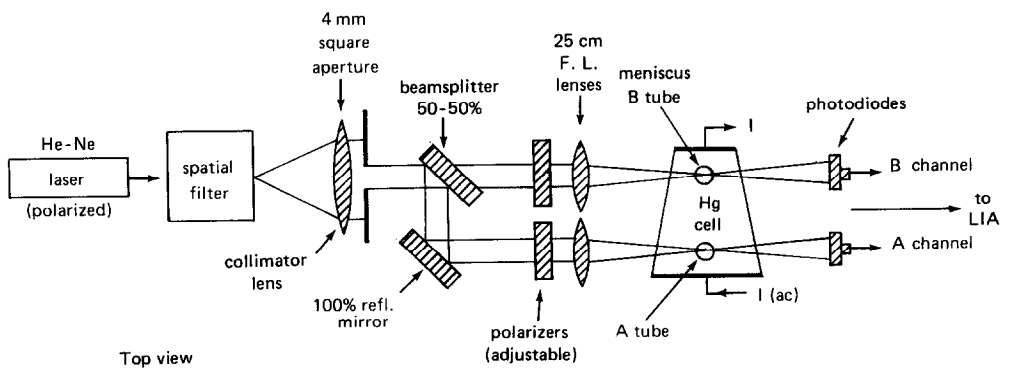

Fig. 2. Schematic of optical amplification method of verifying existence of ponderomotive oscillations of mercury by means of two photodiodes and lock-in amplifier (LIA) capable of monitoring phase relathionships of A and B meniscus motions.

"swinging" mode of oscillation of the mercury (up in one tube when down in the other). Apart from the need to verify ponderomotive transport of mercury there was no advantage in observing both channels. The data reported here were obtained by observing the B channel alone (straight-through beam of fig. 2).

The experiment consists in choosing a fixed frequency f and observing LIA coherent signal S as a function of current I. A computer program determines by least-squares fitting the slope parameter $b(f)$ in the square law, $S=b(f)I^2$, and evaluates the statistics of the fit. This procedure is repeated at a number of frequencies near the resonance frequency f_0. A program then plots the resonance curve of $b(f)$ versus f and determines by least-squares the best three-parameter (a_1, a_2, a_3) fit to the $b(f)$ data among all curves of the type of eq. (7a) in terms of minimizing the statistical chi-squared [7]. Given these fitted a values, the equation of motion parameter values m, R, K are inferred from eq. (7b). Their plausibility is examined and possible alternative explanations of the observations are considered.

4. Calibration

For the procedure just described to yield quantitative results it is necessary to possess values of the parameters k_1, k_2. Wesley's theory, eq. (3a), provides k_2, but k_1 requires calibrating the sensitivity of the optical amplification scheme. Several methods were tried, the most successful of which consisted in immersing in the mercury of tube A or B a vertical wire or small-diameter rod. By changing the immersion depth an amount measured by micrometer, it is possible to infer the change in displaced volume of mercury and in meniscus height. Observation of the change in dc voltage signal across the photodiode load resistor accompanying this known change of meniscus height permits the evaluation of k_1.

A difficulty arose in that not all data exhibited simple proportionality of voltage change of immersion depth change. Consequently all data were subjected to two types of least-squares linear fitting procedures, a one-parameter and a two-parameter fit. (The one-parameter fit evaluates the slope of a best-fitting straight line constrained to pass through the origin. The two-parameter fit evaluates the slope and intercept of a best-fitting straight line not so constrained – only the slope parameter being relevant to the calibration.) Fig. 3 shows an example of immersion calibration raw data in which the two slopes thus obtained are quite similar. In some other cases poorer agreement was obtained. For this reason data were taken for a number of different types of rods

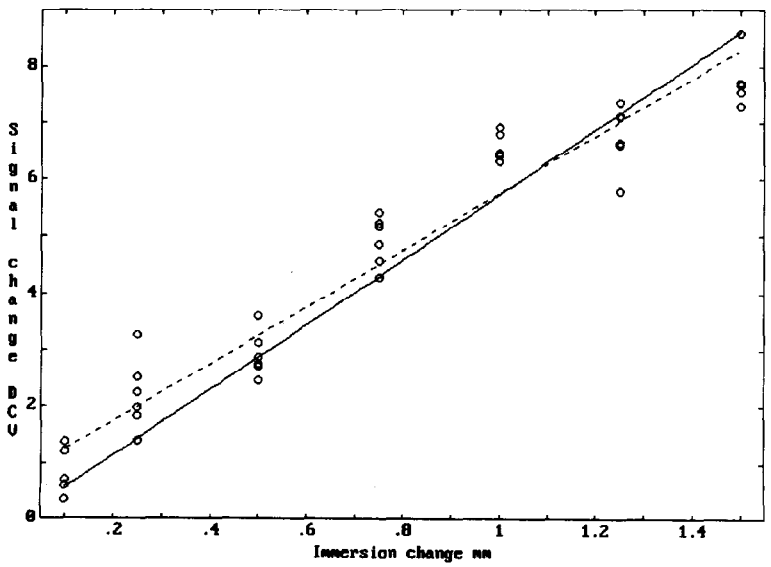

Fig. 3. Example of one-parameter (solid line) and two-parameter (dashed line) least-squares fits of straight lines to 41 data points obtained by recording signal dc level changes accompanying changes of immersion depth in tube B of a 0.0535 inch diameter quartz rod – typical of data obtained by immersion calibration procedure.

and wires with the aim of reducing unknown biases due to peculiarities of any particular case by averaging all results.

The following rods or wires were used (diameter in cm being indicated in parentheses): pyrex rod (0.201), quartz rod (0.136), quartz rod (0.294), #22 nickel wire (0.0644), #22 chromel-A wire (0.0626). The average of all data for these five yielded $k_1 = 6.146 \times 10^6$ for the one-parameter fit and $k_1 = 4.515 \times 10^6$ for the two-parameter fit. Immersions of all rods and wires took place in both the A and B tubes, with observation of signal from the B channel photodiode in all cases. The A and B tube immersion results for a given rod or wire showed rough consistency. Both are included in the averages just cited. Finally, taking the average of the one- and two-parameter fits and letting the discrepancy of this average from either of the averaged values serve as an error indicator (*not* error estimate), we have as a best single figure

$$k_1 (5.33 \pm 0.82) \times 10^6 \text{ (rms mv/rms cm)} . \qquad (8)$$

Since we are dealing with possible unidentified systematic errors, the actual error might conceivably be much greater – the usual "statistical" error analyses being irrelevant.

5. Results

Typical single-frequency data showing LIA signal plotted against the square of rms current (amps) are shown in fig. 4. These are well fit by a one-parameter straight line (constrained to pass through the origin), the slope of which is $b(f) = 0.444$ at $f = 2.3$ Hz, with slope standard deviation $\sigma_b = 0.0051$. The chi-squared of the fit to 21 data points is 52.6, which may be compared with a value of 1375 for the chi-squared of a best one-parameter fit to the same data plotted against current to the first power. It is clear that a square law better describes the data.

Slope values $b(f)$ from current-squared plots similar to that of fig. 4 were evaluated at 13 frequencies in the vicinity of the mechanical resonance frequency $f_0 = 2.21883$ Hz. They are plotted against frequency in fig. 5. The data bar heights show ± 1 standard deviation (σ_b) of the slope data. Clearly a resonance exists. This is the main qualitative point of the experiment. The solid curve in fig. 5 is a least-squares best fitting curve of the form of eq. (7a), obtained by adjusting the three a parameters so as to minimize chi-squared (min $\chi^2 = 99.05$). The resulting best values of these parameters, with their independently inferred 90% confidence intervals [7], are

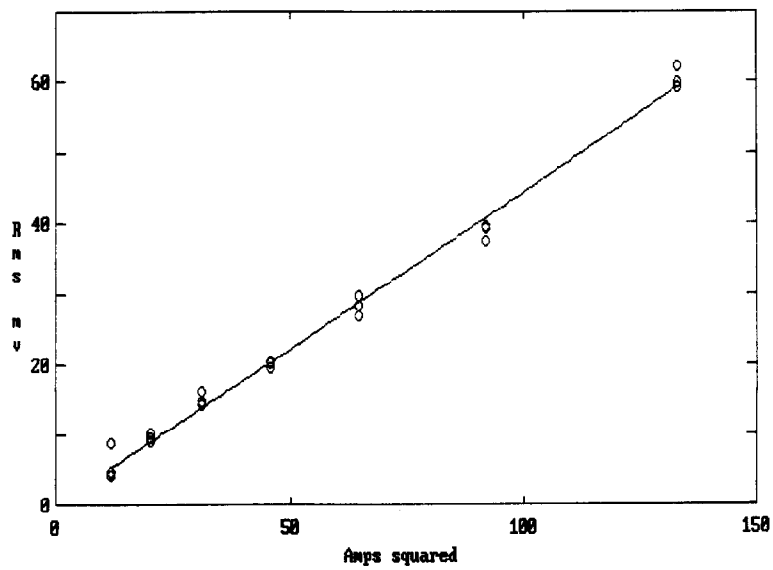

Fig. 4. LIA signal at tuned frequency 2.3 Hz versus I^2 (I = rms amperes). Straight line is best one-parameter least-squares fit to 21 raw data points shown, yielding slope $b = 0.444$ (rms mv/I^2) with slope std. dev. $\sigma_b = 0.0051$. Chi-squared of the fit is 52.6.

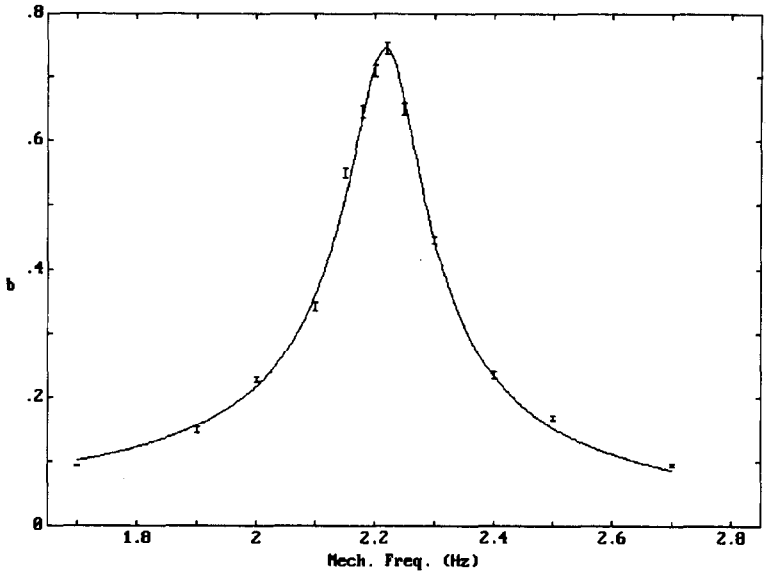

Fig. 5. Resonance curve showing slope parameter $b(f)$ versus frequency f, obtained from single-frequency square-law data plots such as fig. 4, for observations made at 13 frequencies. Bar heights denote ± 1 std. dev. σ_b of b values. Solid curve is best three-parameter fit of the form of eq. (7a), corresponding to minimum $\chi^2 = 99.05$.

$$a_1 = 0.207364 \pm 0.002279\,,$$

$$a_2 = 0.0156874 \pm 0.0005575\,,$$

$$a_3 = 4.92322 \pm 0.00874\,. \qquad (9)$$

Applying eq. (7b), we have three equations in the three unknown physical parameters m, R, K. Accepting the k-values from eqs. (8) and (3a), we get the results tabulated in table 1 under "Observation". The error indicators given there result entirely from the uncertainty in the calibration constant k_1. This possible systematic error overwhelms all other purely "statistical" error sources in the measurements. In particular the a parameter estimated errors of eq. (9) are essentially negligible.

6. Plausibility assessment

To judge the plausibility of the observed results listed in table 1, let us apply elementary physical reasoning. The mass m in motion cannot exceed the total mass of mercury present, about 1500 g. This sets an upper limit, it being likely in view of the cell shape that much of the mercury is stagnant. A lower limit follows from considerations of continuity and in-

Table 1
Equation of motion parameters m, r, K from observation plus eqs. (7b), (9) and as estimated by elementary theory.

Parameter (cgsu)	Elementary theory	Observation (assuming $k_1 = 5.33 \times 10$ (rms mv/rms cm), $k_2 = 0.001511$ (rms dynes/rms amps))
m	$188 < m < 1500$	492 ± 75
R	> 6.3	387 ± 60
K	24410 (for gravity only)	95600 ± 15000

compressibility of the mercury: The moving mass can hardly be less than the mass of mercury contained in the two tubes plus that contained in an imaginary tube of the same diameter lying within the body of the cell and directly joining the two tubes. This consideration leads to an estimated lower limit of 188 g.

Without a detailed fluid dynamical analysis beyond the scope of this inquiry it has not been possible to set meaningful theoretical limits on the dissipation parameter R. If tube wall friction were the only dissipative mechanism, we would have $R=8\pi l\eta$ where η is the viscosity of mercury and l is the effective length of container wall wetted by the moving mercury. Estimating the latter to be about 15 cm, we get $R>6.3$ (cgsu). Obviously some other mechanism of loss predominates – probably turbulence associated with non-streamlined flow within the cell. This speculation cannot be verified here and the question of plausibility of the measured R value must be left open.

The action of the restoring force, gravity, is easily estimated. If the meniscus in one tube rises a distance z above equilibrium level, the incompressibility of mercury implies a fall through distance z in the other tube. The total out-of-equilibrium mass is thus $m^*=2z\pi r_1^2\rho$, where r_1 is tube radius and ρ is mercury density. The force of gravity on this mass is m^*g, and this (if gravity is the sole restoring agent) may be equated to the restoring force Kz in the equation of motion. Thus for $r_1=0.54$ cm we calculate $K=2\pi r_1^2\rho g=24410$ (cgsu). From table 1 it is evident that the agreement with the observed K value is poor. It seems possible that the four times too large restoring force observed in this experiment (table 1) is "real", in the sense that for micron-sized meniscus excursions a contribution of surface tension may be added to that of gravity. Mercury is notable for large surface tension, seven times that of water.

In summary, the plausibility checks in table 1 are satisfactory as to order of magnitude, but suggest the desirability of a less crude theoretical analysis. The indication that about one-third of the mercury mass in the cell participates in the "swinging" oscillation seems inherently reasonable in view of the sharply angular cell geometry. The large value of dissipation constant R observed – far beyond that accounted for by wall friction – indicates that other mechanisms connected with the "lossy" motion of a substantial fraction of the fluid in the cell predominate. The poor check of K values indicates that an accurate quantitative description of the motion will not be possible without more sophisticated analysis. But all observed parameters are seen to be consistent with Wesley's prediction within better than an order of magnitude.

7. Alternative explanations

It may thus be said that to a reasonable (though not quantifiable) degree of confidence the Ampère–Wesley theory is confirmed by observation. This being contrary to currently widely held opinions about the nature of physical forces, we must weigh alternative explanations for what has been observed:

(1) *A heating effect is responsible for the observations.* This is ruled out by the facts that (a) the mercury cell was maintained during all observations in a large Dewar vessel at the temperature of melting ice, (b) the electrical resistance of the cell is below 0.01 ohm and the currents used never exceeded 11.6 amps rms. No detectable heat generation occurred within the cell.

(2) *An inductive effect is responsible.* This is implausible since mechanical oscillation frequencies never exceeded 2.7 Hz, meaning electrical frequencies not over 1.35 Hz. The experiment was therefore a quasi-static one.

(3) *Some effect of paramagnetism is at work.* Again implausible, since the susceptibility of mercury is not excessive, about like that of silver.

(4) *The Lorentz force is operative and produces an observable "pinch" effect.* This seems plausible because pinch forces vary with the square of current. The explanation fails in two ways: (i) Quantitatively – the pinch forces at such low currents being too small by at least an order of magnitude. (ii) Qualitatively, in that observed forces are ponderomotive – that is, they act on the positive ions of the mercury to produce mass transport. The only ponderomotive effects of the Lorentz (radial pinch) force are such as to press the ions closer to the central axis of current flow ... and such compression is limited in its *observability* by the small compressibility of mercury (which we have elsewhere chosen to neglect).

There is of course no *direct* Lorentz force on the ions, because they are at least initially (on the average) at rest in the laboratory, $v=0$, so the Lorentz force on the, $v\times B$, vanishes. (Even the small compressibility effect just mentioned is produced indirectly, through electromotive action on the electrons, which then act Coulombically on the ions.) The observed meniscus excursions, of the order of microns, would require kilograms of force if effected by compressibility, not the fractions of a dyne available at these currents.

(5) *The Lorentz force is operative and acts through the radial rather than longitudinal components of current flow within the cell.* Such an explanation cannot be entirely ruled out for the geometry of this experiment. It could be ruled out by cell redesign to reduce the sharpness of taper in the longitudinal direction. As it is, the sloping (convergence/divergence) of current flow lines implies that forces transverse to the current elements possess a small longitudinal component – so it is not true that the Lorentz force law implies zero longitudinal action. In general magnetic forces cause motion in the fluid, mathematically speaking curl$(J\times B)$ is not zero in general. Workers in fusion research have found it very difficult to attain the equilibrium case in 40 years of research. Unlike radial (pinch) forces, longitudinal forces do not have to work against the compressibility of mercury, but only against the force of gravity and surface tension at the free surfaces in the vertical tubes. However, the effect is at least an order of magnitude smaller than the Ampère force ... so this avenue of escape looks unpromising.

(6) *Some unknown physical effect or attribute of current-carrying mercury causes it to mimic Ampère force law behavior*, thereby hiding the fact that the true law of action is Lorentz's. This hypothesis is not disprovable but is scientifically acceptable only as a prelude to further investigation (to be conducted by the hypothesizer).

8. Summary

(1) In an ac version of the Wesley mercury experiment mass transport between tubes of the cell has been verified by observing 180° phase differences between the coherent LIA signals associated with the two tubes. When one meniscus moves up the other moves down. The presence of current-induced ponderomotive forces is thus confirmed.

(2) The variation of these forces with the square of current passing thorough the cell is indicated by the detection of coherent LIA signal at a tuned frequency twice that of the applied e.m.f.

(3) This square-law variation is explicitly confirmed by data such as those of fig. 4 showing satisfactory statistical fits to a square law for ac varying between 1 and 11.6 amps rms.

(4) The existence of a resonance, fig. 5, confirms the implication of the foregoing that Ampère forces have been observed. This conclusion is reinforced by the difficulty noted in the preceding section of finding an alternative explanation based on known physical fact.

(5) The theory of Ampère is semi-quantitatively confirmed – insofar as the limited refinement of the experiment allows. Wesley's calculation [5] assumes the validity of the Ampère force law, eq. (1), and leads to a force constant $k_2=0.001511$ (rms dynes/(rms amps)^2). This order of magnitude is consistent with the observations.

(6) It is concluded that there are sufficiently firm grounds for inference that the action of Ampère forces has been observed to motivate further investigation. Such forces, being of noncovariant form, violate spacetime symmetry.

Acknowledgement

We thank J.A. Saldeen, C.J. Hawley Jr. and J. Wentz of the University of Illinois Chemistry Department for vital electronic help, without which the experiment would have been impossible; D. O'Brien and co-workers for glass-blowing assistance; and R.I. Gray, D.E. McLennan and other readers for helpful criticism.

References

[1] P. Graneau, Ampère–Neumann electrodynamics of metals (Hadronic Press, Nonantum, MA, 1985).
[2] E.T. Whittaker, A history of the theories of aether and electricity, Vol. 1 (Harper, New York, 1960).

[3] J.C. Maxwell, A treatise on electricity and magnetism, Vol. 1 (Clarendon, Oxford, 1891; Dover, New York, 1954) p. 319.
[4] C. Christodoulides, Am J. Phys. 56 (1988) 357; J. Phys. A 20 (1987) 2037.
[5] J.P. Wesley, in: Progress in space-time physics (Benjamin Wesley, 7712 Blumberg, FRG, 1987) pp. 187–190.
[6] P.M. Morse, Vibration and sound (McGraw-Hill, New York, 1936).
[7] W.H. Press, B.P. Flannery, S.A. Teukolsky and W.T. Vetterling, Numerical recipes (Cambridge Univ. Press, Cambridge, 1987).